Expression of heteromeric amino acid transporters along the murine intestine

Mital H. Dave, Nicole Schulz, Marija Zecevic, Carsten A. Wagner and Francois Verrey

Institute of Physiology, University of Zurich, Zurich, Switzerland

Members of the new heterodimeric amino acid transporter family are composed of two subunits, a catalytic multitransmembrane spanning protein (light chain) and a type II glycoprotein (heavy chain). These transporters function as exchangers and thereby extend the transmembrane amino acid transport selectivity to specific amino acids. The heavy chain rBAT associates with the light chain $b^{\circ,+}AT$ to form a cystine and cationic amino acid transporter. The other heavy chain, 4F2hc, can interact with seven different light chains to form various transporters corresponding to systems L, y^+L, asc or x^-_c. The importance of some of these transporters in intestinal and renal (re)absorption of amino acids is highlighted by the fact that mutations in either the rBAT or $b^{\circ,+}AT$ subunit result in cystinuria whereas a defect in the y^+-LAT1 light chain causes lysinuric protein intolerance. Here we investigated the localization of these transporters in intestine since both diseases are also characterized by altered intestinal amino acid absorption. Real time PCR showed organ-specific expression patterns for all transporter subunit mRNAs along the intestine and Western blotting confirmed these findings on the protein level. Immunohistochemistry demonstrated basolateral coexpression of 4F2hc, LAT2 and y^+-LAT1 in stomach and small intestine, whereas rBAT and $b^{\circ,+}AT$ were found colocalizing on the apical side of small intestine epithelium. In stomach, 4F2hc and LAT2 were localized in H^+/K^+-ATPase-expressing parietal cells. The abundant expression of several members of the heterodimeric transporter family along the murine small intestine suggests their involvement in amino acids absorption. Furthermore, strong expression of rBAT, $b^{\circ,+}AT$ and y^+-LAT1 in the small intestine explains the reduced intestinal absorption of some amino acid in patients with cystinuria or lysinuric protein intolerance.

Prior to absorption, proteins are first degraded in the stomach and the small intestine into small oligopeptides and amino acids. Small peptides consisting of two or three amino acids can be absorbed across the apical membrane of the enterocytes lining the small intestine via the H^+-driven peptide transporter PEPT-1 and are then mostly broken down intracellularly into single amino acids (Groneberg *et al.* 2001; Daniel & Rubio-Aliaga, 2003). In contrast, amino acids are transported across the apical membrane by several transport systems as characterized functionally in earlier work using either stripped intestinal mucosa or isolated brush border membrane vesicles (Munck, 1995; Munck & Munck, 1999; Munck *et al.* 2000; Torras-Llort *et al.* 2001). Several distinct transport systems have been identified based on their ion dependence (i.e. Na^+ and/or Cl^- dependence) and their profile of amino

acids accepted (Munck, 1995; Munck *et al.* 2000; Palacin *et al.* 1998). The main amino acid transport systems described on the apical brush border membrane are the Na^+-dependent neutral amino acid transport system B^0 (Munck & Munck, 1999; Munck *et al.* 2000), the Na^+-dependent system for neutral and dibasic amino acids $B^{0,+}$ (Munck, 1995), the Na^+ and K^+-dependent system X^-_{AG} for anionic amino acids (Munck *et al.* 2000), the H^+-driven system PAT (possibly system IMINO) for proline and glycine (Chen *et al.* 2003), the Na^+-dependent system ASC for alanine, serine and cysteine (Munck & Munck, 1999; Munck *et al.* 2000; Avissar *et al.* 2001), and the Na^+-independent system $b^{\circ,+}$ for neutral and dibasic amino acids (Munck *et al.* 2000; Torras-Llort *et al.* 2001; for review: Munck, 1995; Palacin *et al.* 1998). Following uptake into enterocytes, amino acids are then released

into the extracellular space and blood on the basolateral side, completing their intestinal absorption. Also on the basolateral side, functionally distinct amino acid transport systems have been identified. The Na^+-dependent systems A and N for alanine and glutamine (Wilde & Kilberg, 1991), the Na^+-dependent system y^+L for dibasic amino acids (Desjeux *et al.* 1980), and the Na^+-independent systems asc and L for small and larger neutral amino acids (Lash & Jones, 1984; Wilde & Kilberg, 1991). Whereas the molecular identity and regulation of peptide transporters and some Na^+-dependent amino acid transporters on the apical membrane has been elucidated over the last decade (Palacin *et al.* 1998), little has been known about the molecular identity of Na^+-independent amino acid transport systems involved in both the apical uptake and basolateral release into blood.

Recently, a novel family of heteromeric amino acid transporters has been identified on a molecular level and functionally characterized in heterologous expression systems (for review: Verrey *et al.* 2000; Chillaron *et al.* 2001; Wagner *et al.* 2001, 2004; Palacin & Kanai, 2004). Heteromeric amino acid transporters are structurally distinguished from other families by their dimeric composition of two subunits, a heavy and a light chain. The heavy chains (4F2hc (SLC3A2) and rBAT (SLC3A1)) are glycosylated type II membrane proteins which are mainly involved in the trafficking and stabilization of the associated light chains (Palacin & Kanai, 2004). In contrast, the light chains (LAT1, LAT2, y^+-LAT1, y^+-LAT2, Asc-1, xCT, and $b^{\circ,+}AT$ (SLC7A5-11)) are classic polytopic membrane proteins with postulated 12 transmembrane domains which confer the specificity of the expressed transport systems (for review: Verrey *et al.* 2004).

Functionally, heteromeric amino acid transporters mostly obey an antiport mechanism leading to exchange of amino acids (Verrey *et al.* 2004). Based on a one-to-one stoichiometry as demonstrated for system $b^{\circ,+}$, y^+L and L (Chillaron *et al.* 1996; Meier *et al.* 2002), heteromeric amino acid transporters are not themselves performing net transport of amino acids but seem to broaden the selectivity range of the amino acid transport that is driven by Na^+-dependent or other directional amino acid transporters expressed in parallel (Verrey *et al.* 2000; Broer, 2002). System $b^{\circ,+}$ ($b^{\circ,+}AT$ and rBAT) mediates apical uptake of dibasic amino acids and cystine in exchange for intracellular neutral amino acids. System L (4F2hc and LAT1 or LAT2) releases basolaterally smaller intracellular neutral amino acids in exchange for larger extracellular neutral amino acids, whereas system y^+L (consisting of 4F2hc and y^+-LAT1 or y^+-LAT2) releases intracellular

dibasic amino acids in exchange for extracellular neutral amino acids together with Na^+ (Wagner *et al.* 2001; Broer, 2002; Verrey *et al.* 2004). The systems x^-_c (4F2hc and xCT) and asc (4F2hc and Asc-1) mediate exchange of intracellular glutamate against anionic cystine and the transport of alanine, serine and cysteine, respectively (Wagner *et al.* 2001; Broer, 2002; Verrey *et al.* 2004).

Mutations in either rBAT or $b^{\circ,+}AT$ result in cystinuria, an autosomal recessive hereditary disorder characterized by the renal loss of dibasic amino acids and cystine associated with the impaired absorption of these amino acids in the small intestine (Calonge *et al.* 1994; Feliubadalo *et al.* 1999; Palacin *et al.* 2001). The more severe disease lysinuric protein intolerance (LPI), caused by mutations in the y^+-LAT1 (SLC7A7) catalytic subunit, is also characterized by the renal loss and impaired intestinal absorption of dibasic amino acids. It also causes several metabolic abnormalities that reduce the life-expectancy of patients dramatically (Borsani *et al.* 1999; Torrents *et al.* 1999; for review: Simell, 2001).

In order to better understand the role of heteromeric amino acid transporters in normal intestinal function and in the pathophysiology of cystinuria and lysinuric protein intolerance, we examined the segmental and subcellular localization as well as the relative abundance of these transporters along the mouse intestine using real time PCR, Western blotting, and immunohistochemistry. In addition, the exact localization of expression of this family of amino acid transporters may also allow future investigation of adaptive processes under physiological conditions or in animal models of cystinuria or lysinuric protein intolerance.

Methods

This study used male NMRI mice of 12 weeks of age, 25–30 g. They were killed by I.P. injection of ketamine–xylazine and subsequent cervical dislocation, and organs were rapidly harvested. Animal handling was according to the Swiss Animal Welfare laws and approved by the Kantonales Veterinäramt Zürich.

Real-time PCR

RNA extraction and reverse transcription. NMRI mice were killed and tissues were collected and rapidly frozen until further use. Stomach, duodenum, jejunum, ileum and colon were identified, cleansed several times in ice-cold phosphate-buffered saline (PBS) and the mucosa cell layers were scraped off on ice and rapidly frozen. The duodenum was identified as proximal to the ligament

of Treitz (first 2 cm), the jejunum as the upper part (upper 2/5) of the small intestine distal to the ligament of Treitz and the ileum as the lower part (lower 2/5) of the small intestine ending before the caecum. Between the duodenum and jejunum, 5 cm of tissue was removed as a safety margin as well as 10 cm between the jejunum and ileum. The total colon was used for mucosa isolation. Total mRNA was extracted from 30 mg of mucosal tissue using the RNA Aqueous 4PCR kit (Ambion) according to the manufacturer's instructions. For RNA extraction, mucosal tissue was thawed in RNALater solution (Ambion), transferred to lysis buffer and homogenized on ice with a Potter-Elvehjem tissue grinder. RNA was bound on columns and treated with DNAse for 15 min at 30°C to reduce genomic DNA contamination. Quantity and purity of total eluted RNA was assessed by spectrometry and on agarose gels. Each RNA sample was diluted to 200 ng μl^{-1} and 1 μl used as template for reverse transcription using the Taqman Reverse Transcription kit (Applied Biosystems, Foster City, CA, USA).

For reverse transcription, 200 ng RNA template was diluted in a 20 μl reaction mix that contained (final concentrations): RT buffer ($1\times$), $MgCl_2$ (5.5 mM), random hexamers (2.5 μM), RNAse inhibitor (0.4 U μl^{-1}), the multiscribe reverse transcriptase enzyme (1.25 U μl^{-1}), deoxyNTP mix (500 μM each) and RNAse free water.

Real time PCR. Real-time PCR was performed as previously described (Loffing *et al.* 2001) according to the recommendations supplied by Applied Biosystems (http://home.appliedbiosystems.com). Primers for all genes of interest were designed using Primer Express software from Applied Biosystems (see Table 1). Primers were chosen to result in amplicons of 70–150 bp that span intron–exon boundaries to avoid the effect of potentially contaminating genomic DNA. The specificity of all primers was first tested on mRNA derived from several tissues and resulted always in a single product of the expected size (data not shown). Probes were labelled with the reporter dye FAM at the 5′ end and the quencher dye TAMRA at the 3′ end (Microsynth, Balgach, Switzerland). The passive reference dye (ROX) was included in the Taqman buffer supplied by the manufacturer. Twenty microlitres of cDNA obtained from the RT reaction was diluted to 100 μl with RNAse free water. A 25 μl PCR reaction volume was prepared using 5 μl diluted cDNA as template with sense and antisense primers (25 μM each) and the labelled probe (5 μM). The Taqman Universal PCR Master Mix (Applied Biosystems) was added to the final volume. Prior quantification experiments had

determined the optimal concentrations of primers and probes and temperature settings in order to yield maximal fluorescence signals and PCR products. Reactions were run in 96-well optical reaction plates using a Prism 7700 cycler (Applied Biosystems). Thermal cycles were set at 95°C (10 min) and then 40 cycles at 95°C (15 s) and 60°C (1 min) with auto ramp time. For analysing the data, the threshold was set to 0.06 as this value had been determined to be in the linear range of the amplification curves for all mRNAs in all experimental runs. All reactions were run in duplicate. The abundance of the target mRNAs was calculated relative to a reference mRNA (glyceraldehyde 3-phosphate dehydrogenase, GAPDH). Since standard curves made for all primer pairs on jejunum RNA had revealed an efficiency value close to 2 (fold-increase in input mRNA required to decrease the cycle number by 1), relative expression ratios were calculated as $R = 2^{(\text{Ct(GAPDH)}-\text{Ct(test)})}$, where Ct is the cycle number at the threshold and test stands for the tested mRNA.

Western blotting

NMRI mice were killed and organs rapidly harvested. Animal handling was according to the Swiss Animal Welfare laws and approved by the Kantonales Veterinäramt Zürich. Stomach, duodenum, jejunum, ileum, and colon were identified, cleansed several times in ice-cold PBS and the mucosa cell layers were immediately scraped off on ice and transferred into ice-cold K-Hepes buffer (200 mM mannitol, 80 mM K-Hepes, 41 mM KOH, pH 7.5) with pepstatin, leupeptin, K-EDTA, and phenylmethylsulphonyl fluoride (PMSF) added as protease inhibitors. The samples were homogenized with a tip sonicator, centrifuged at 1000 g for 10 min at 4°C and the supernatant saved. Subsequently, the supernatant was centrifuged at 100 000 g for 1 h at 4°C and the resultant pellet resuspended in K-Hepes buffer containing protease inhibitors. After measurement of the total protein concentration (Bio-Rad Protein Kit), 50 μg of crude membrane protein were solubilized in Laemmli sample buffer, and SDS-Page was performed on 10 and 12% polyacrylamide gels. For immunoblotting, proteins were transferred electrophoretically from unstained gels to polyvinylidene difluoride (PVDF) membranes (Immobilon-P, Millipore, Bedford, MA, USA). After blocking with 5% milk powder in Tris-buffered saline–0.1% Tween-20 for 60 min, the blots were incubated with the primary antibodies and mouse monoclonal anti-actin (42 kDa, Sigma) 1 : 500 either for 2 h at room temperature or overnight at 4°C. The primary

Table 1. Primers and probes used for real-time PCR

Gene	Primers	Probe	Acc. no.
SLC3A1 (rBAT)	S: 5′-TGGAAGCGAAGGATCTGAGAA (1001–1021)[1] A. 5′-GCTCTGAGTAGTGGGTGACCG (1058–1078)	5′-AAATCCAAGTGAATACATCCCAAATTCCGGA (1025–1055)	D88533.1
SLC3A2 (4F2hc)	S: 5′-GTTTTTGAATGCCACTGGCA (1073–1092) A: 5′-GTCCTGAGGAGCGTCTGAAA (1123–1142)	5′-ATGGTGCAGCTGGAGTGTGTCGCA (1097–1120)	NM008577.1
SLC7A5 (LAT-1)	S: 5′-TTTGCTTGGCTTCATCCAGAT (665–685) A: 5′-TTGGACGTBTACTTCAACAGG (717–737)	5′-AAGGACATGGGACAAGCTGATGCGTC (690–715)	AB017189.1
SLC7A6 (y⁺-LAT-2)	S: 5′-TACATCCTGACCAACGTGGC (894–913) A: 5′-ATGCCGAATGTCTGGTCAGC (975–994)	5′-TCCATAAGAGTGACGCTGTGCCTGTGA (943–969)	BC038404
SLC7A7 (y⁺-LAT-1)	S: 5′-ATTCCAGTAGCGGTTGCATTC (1186–1206) A: 5′-GAGCTCTCTTCCGGTGGAGG (1266–1284)	5′-TTGCTTTGGTGGGCTCAACGCC (1209–1230)	NM 011405
SLC7A8 (LAT-2)	S: 5′-TCCACGTTTGGTGGAGTCAA 1529–1548 A: 5′-TCACACAACCGGTACTAGGT (1610–1629)	5′-CTCCCTCTTCACCTCCTCCCGGCT (1552–1575)	NM 016972
SLC7A9 (b⁰,⁺AT)	S: 5′-GCTCTTGCAGTCCCAGGC T (1172–1190) A: 5′-GGGACTACCCAAGATGCTGGA (1223–1243)	5′-CTGTGACCTTCGGAGACCGCGTTCT (1195–1219)	NM 021291
SLC7A10 (ascAT-1)	S: 5′-TGTCAGACGCTGCACCC (1103–1119) A. 5′-ACGAGCATGATGACCGCTG (1153–1171)	5′-TGCCCTCCTTGTCTGTTGCGGG (1127–1149)	AB026688.1
SLC7A11 (xCT)	S: 5′-TGGAACTGCTCGTAATACGCC (705–725) A: 5′-GGTTCCAGGATGTAGCGTCC (758–777)	5′-TGGAGCTACTGCTGTGATATCCCTGGCAT (727–755)	AB022345.1
GAPDH	S: 5′-GTCGTGGATCTGACGTGCC (764–782) A: 5′-GATGCCTGCTTCACCACCTT (818–837)	5′-CCTGGAGAAACCTGCCAAGTATGATGACAT (784–813)	M32599

Primers and probes used for real-time PCR. All primers and probes were designed using Primer Express software from Applied Biosystems. All probes are spanning intron-exon boundries to exclude genomic DNA contamination. Primers were tested using RT-PCR and only primers yielding a single band of the expected size were used for subsequent real-time PCR experiments. The nucleotide numbers of the primers and probes are given in brackets.

antibodies were: rabbit anti-rat LAT-1 (affinity purified antibody 200 μg ml^{-1}, 1 : 2000, kind gift of N. Thompson, Brown University, RI, USA; Campbell *et al.* 2000), rabbit anti-mouse LAT-2 (serum 560, 1 : 2000; Rossier *et al.* 1999), rabbit anti-mouse y⁺-LAT-1 (affinity purified antibody 398, 1 : 500; Bauch *et al.* 2003), rabbit anti-mouse b⁰,⁺AT (sera 400 and 558, 1 : 2000; Pfeiffer *et al.* 1999), and goat anti-rabbit 4F2hc (200 μg ml^{-1}, 1 : 1000; Santa Cruz Biotechnology, Santa Cruz, CA, USA). After washing and subsequent blocking, blots were incubated with secondary antibodies conjugated with alkaline phosphatase (goat anti-rabbit 1 : 5000 and donkey anti-goat 1 : 5000; Promega, Madison, WI, USA), for 1 h at room temperature. Antibody

binding was detected with the CDP Star kit (Roche Diagnostics Corp., Indianapolis, IN, USA) before exposure to X-ray film (Kodak). The specificity of the antibodies used was tested using pre-incubation with the immunizing peptides and pre-immune sera (data not shown).

Immunohistochemistry

NMRI mice were anaesthetized and perfused through the left ventricle with PBS followed by paraformaldehyde–lysine–periodate (PLP) fixative (McLean & Nakane, 1974). Kidneys and small and large intestines were removed, flushed with fixative solution and postfixed overnight at 4°C by immersion in PLP. Organs were washed three times with PBS and 5 μm cryosections were cut after cryoprotection with 2.3 M sucrose in PBS for at least 12 h. For immunostaining, tissues were taken from kidney, stomach (fundus and corpus), duodenum, jejunum, ileum, and proximal and distal colon. Immunostaining was carried out as previously described (Wagner *et al.* 2002). Briefly, sections were incubated with 1% SDS for 5 min, washed 3 times with PBS and incubated with PBS containing 1% bovine serum albumin for 15 min prior to the primary antibody. The primary antibodies (see Western blotting) were diluted in PBS at dilutions of 1 : 200 to 1 : 1000 and applied either for 75 min at room temperature or overnight at 4°C. Sections
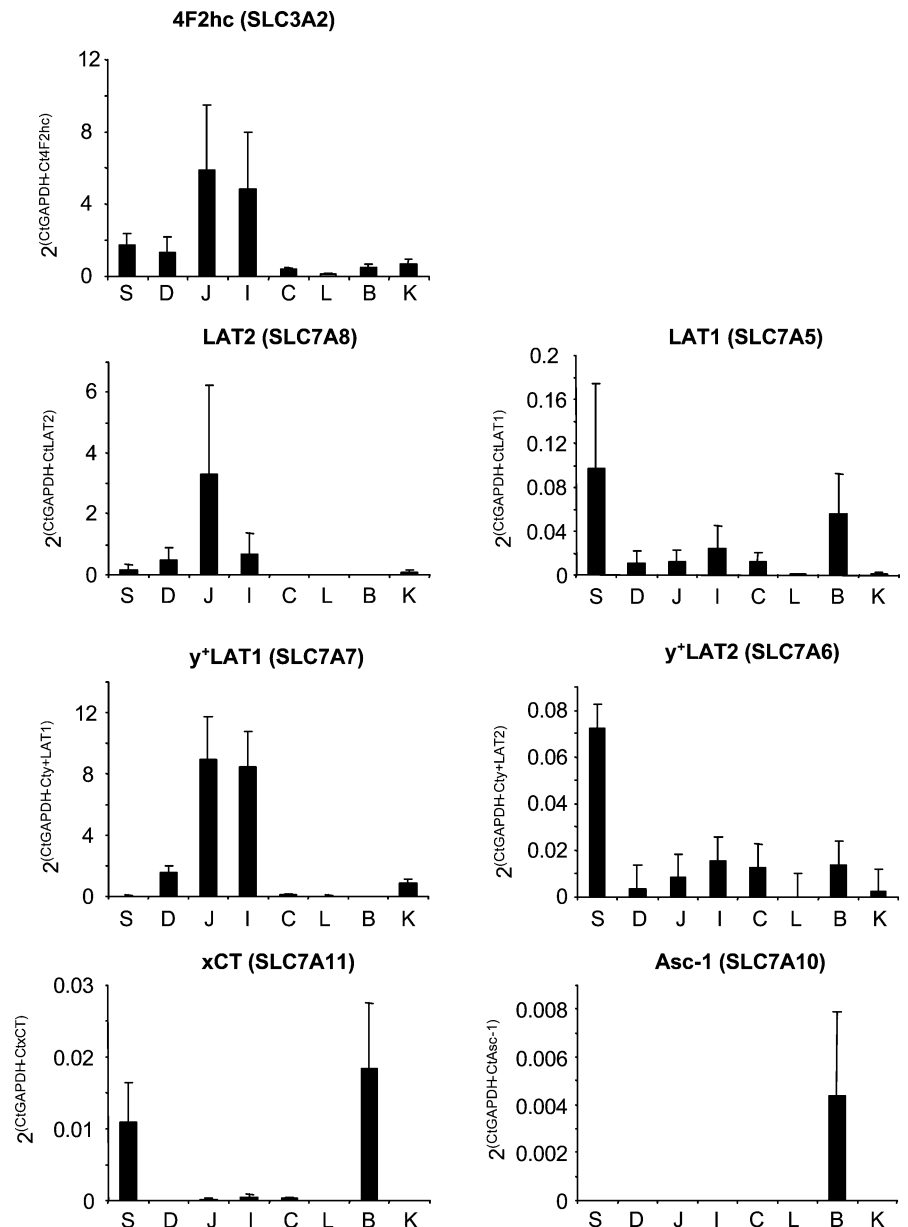

Figure 1. Relative mRNA abundance of 4F2hc and associated light chains
The abundance of the different test mRNAs relative to that of GAPDH ($2^{(Ct(GAPDH)-Ct(TEST))}$ is indicated for each tissue tested (see Methods). 4F2hc mRNA showed a wide tissue distribution with a segmental gradient of expression in small intestine that is similar to that of LAT2 and y$^+$-LAT1. The mean relative mRNA abundance tested independently in three mice is shown. S, stomach; D, duodenum; J, jejunum; I, ileum; C, colon; L, liver; B, brain; K, kidney.

were then washed twice for 5 min with high-NaCl PBS (PBS + 2.7% NaCl) and once with PBS, and incubated with the secondary antibodies (donkey anti-rabbit, donkey anti-mouse, and donkey anti-goat at dilutions of 1 : 1000, 1 : 400, and 1 : 400, respectively) for 1 h at room temperature. Sections were again washed twice with high-NaCl PBS and once with PBS before mounting with VectaMount (Vector Laboratories, Burlingame, CA, USA). Sections were viewed with a Nikon ECLIPSE TE 300/200 inverted microscope or a Leica SP1 UV CLSM confocal microscope. Pictures were processed and assembled using Adobe Photoshop. All antibodies were tested for their specificity using pre-immune sera and immunizing peptides. The secondary antibodies alone did not result in significant staining (data not shown).

Results

Distribution of heteromeric amino acid transporter mRNAs

Real-time PCR was used to assess the relative abundance of mRNA of all members of the heteromeric amino acid transporter family comprising rBAT or 4F2hc in the epithelial layer of stomach, small intestine and colon. As internal standard, GAPDH mRNA was measured
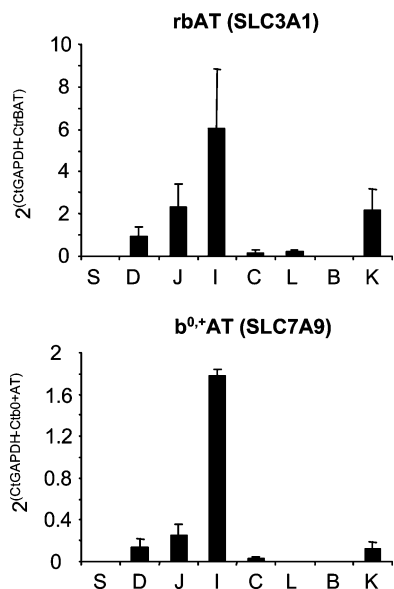

Figure 2. Relative mRNA abundance of rBAT and $b^{\circ,+}$AT
The mRNA abundance relative to GAPDH was calculated as in Fig. 1. Significant expression was only found in kidney, duodenum, jejunum and ileum with a strong segmental gradient and a highest relative expression level in ileum. rBAT and $b^{\circ,+}$AT mRNAs showed a parallel expression that resembles that of LAT2 and y^+-LAT1. Means from three mice are shown. S, stomach; D, duodenum; J, jejunum; I, ileum; C, colon; L, liver; B, brain; K, kidney.

in all samples and values obtained for test mRNAs were normalized against it similarly to what has been previously described (Loffing *et al.* 2001) (see Methods). Brain, kidney and liver RNAs were also included for comparison, since these organs are known to express substantial levels of all amino acid transporter subunits tested here (Wagner *et al.* 2001). These experiments revealed the presence of mRNAs coding for all tested subunits in mouse intestine, but with distinct amounts and patterns of distribution (Figs 1 and 2). Several interesting observations were made: (i) the mRNAs encoding subunits of amino acid transporters implicated in the transepithelial transport of amino acids in (re)absorptive tissues (rBAT, $b^{\circ,+}$AT, 4F2hc, LAT2, y^+-LAT1) were mainly expressed in the small intestine and kidney with the exception of LAT2 and 4F2hc; (ii) the main sites of mRNA expression of absorptive amino acid transporters were the jejunum and the ileum; (iii) substantial levels of mRNA for the LAT2 subunit, the catalytic subunit of a transporter thought to play an important role in amino acid (re)absorption, was found in stomach, an organ not previously recognized as a major site of amino acid absorption; (iv) substantial mRNA levels of xCT, the catalytic subunit of a transporter implicated in stress reactions or protection against oxidative stress, were found in stomach; (v) LAT1, xCT and Asc-1 mRNAs were most abundant in brain and low in intestine (but in stomach for xCT and LAT1); and (vi) mRNA levels of y^+-LAT2 were low in all tissues tested but highest in stomach.

Distribution of heteromeric amino acid transporter proteins

The expression of heteromeric amino acid transporter subunit proteins was investigated by Western blotting. As expected from the mRNA data, the heavy chain 4F2hc was expressed all along the small intestine, strongly in stomach, jejunum and ileum, less in duodenum and only weakly in colon. In contrast, LAT1 was not detected in intestine, but gave a strong signal in brain (Fig. 3). The protein expression levels of the (re)absorptive amino acid transporter catalytic subunits $b^{\circ,+}$AT, LAT2 and y^+-LAT1 followed the pattern observed for the corresponding mRNAs. $b^{\circ,+}$AT protein was found only in kidney and the small intestine with little expression in duodenum and high levels of expression in jejunum and ileum. Similarly, expression of y^+-LAT1 was seen only in kidney and small intestine, with highest levels in jejunum and ileum. The pattern of LAT2 protein expression confirmed the results from real-time PCR

showing surprisingly high levels of LAT2 protein in stomach. In the small intestine, LAT2 protein was found in all three segments with highest levels again in jejunum and ileum. As mentioned above, the associated heavy chain 4F2hc showed a localization pattern that resembles that of LAT2. The xCT, Asc-1 and rBAT subunit proteins could not be detected by Western blotting because of lack of specific antibodies.

Segmental and subcellular localization of heteromeric amino acid transporters

Immunohistochemistry was used to investigate the segmental and subcellular localization of heteromeric amino acid transporter subunits in stomach, small intestine and colon. In mouse stomach, anti-LAT2 serum showed strong basolateral staining in large bulging cells resembling the acid-secretory parietal cells. 4F2hc

colocalized with LAT2 in these cells (Fig. 4). In order to identify parietal cells, a coimmunostaining for LAT2 and the parietal cell specific β-subunit of the gastric H^+/K^+-ATPase was performed. LAT2 localized exclusively to cells positive for the gastric H^+/K^+-ATPase, but at their other pole, demonstrating the basolateral localization of LAT2 and 4F2hc in parietal cells (Fig. 4). In duodenum, jejunum and ileum, a strong LAT2 and 4F2hc signal was seen on the basolateral side of enterocytes lining the lumen. The signal showed a strong gradient along the length of the villi, being stronger towards the tip of the villi and almost invisible in the crypts between the villi. 4F2hc and LAT2 colocalized completely in all segments of the small intestine and along the length of the villi (Fig. 5). However, not all cells lining the lumen of the small intestine were stained for 4F2 and LAT2 consistent with the presence of other cells such as mucus or endocrine cells. Also, there was a notably stronger staining for 4F2hc towards the base
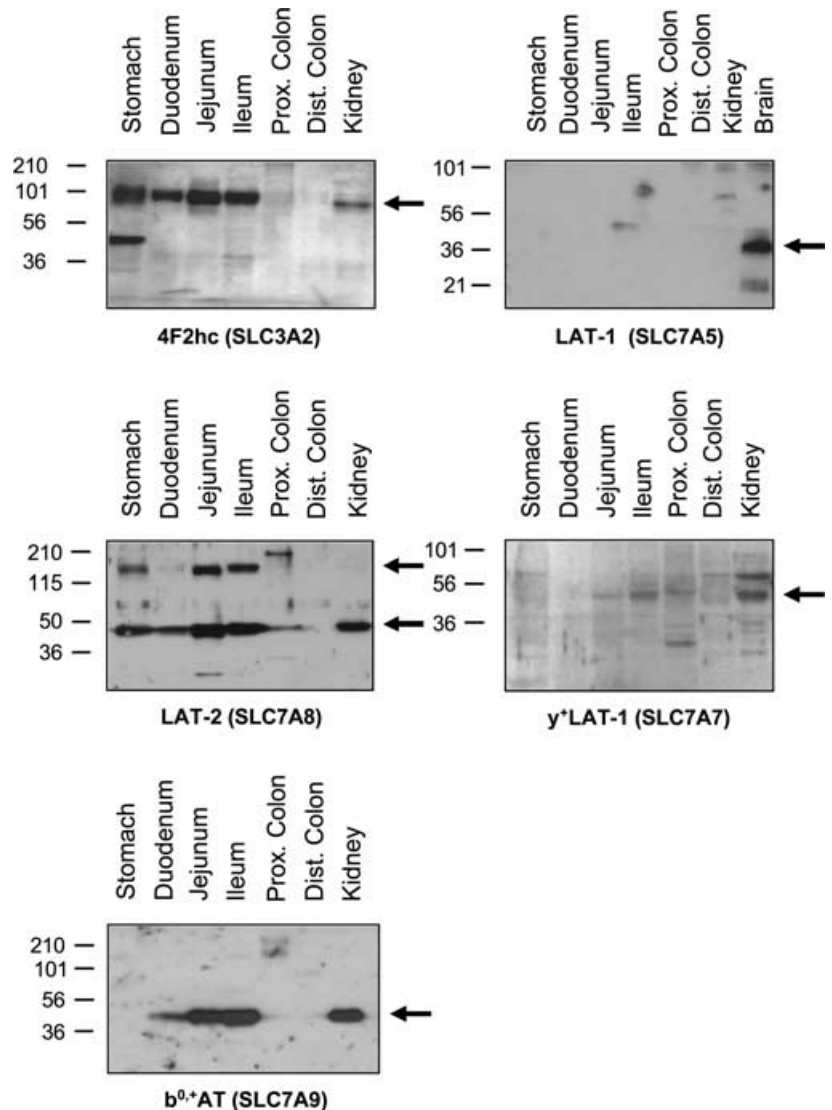

Figure 3. Protein abundance of heteromeric amino acid transporters

The segmental expression and abundance of 4F2hc (migrating at ~80 kDa), of its associated light chains LAT1, LAT2 and y$^+$-LAT1 (~35–45 kDa) as well as of the rBAT-associated light chain b$^{\circ,+}$AT was assessed by Western blotting (50 μg crude membrane protein per lane). Kidney and brain were loaded as control. As for mRNA, distinct patterns of protein expression were found for all subunits assayed. LAT1 was found only in brain. LAT2 showed a gradient of expression along the small intestine but was also abundant in stomach. For LAT2 a second band of higher molecular weight (approx. 120–150 kDa) was seen which was specific and may represent the heterodimer formed together with 4F2hc. y$^+$-LAT1 expression was confined to the small intestine and kidney and increased along the small intestine. b$^{\circ,+}$AT showed a similar pattern of expression to y$^+$-LAT1. Western blots shown represent data from one representative mouse but qualitatively similar results were obtained from three different mice in separate experiments.

of the villi as for LAT2 suggesting different intensities or gradients of expression. No LAT2-specific staining was found in colon (Supplementary material, Fig. 1). Also, y^+-LAT1 colocalized with 4F2hc to the basolateral membrane of enterocytes in duodenum, jejunum and ileum (Fig. 6). The staining was very weak in the duodenum in agreement with only low mRNA and protein expression levels in this segment. Similar to LAT2, y^+-LAT1 showed a strong gradient of expression along the length of the villi with stronger expression towards the tip of the villi and not all cells were positive for y^+-LAT1 staining (Fig. 6). Towards the base of the villi a less complete colocalization of 4F2hc and y^+-LAT1 was observed, possibly due to differences in relative abundance (Fig. 6*I*). No y^+-LAT1 staining was found in stomach or colon (Supplementary material, Fig. 2). In contrast to 4F2hc, LAT2 and y^+-LAT1 that localized basolaterally, rBAT and $b^{\circ,+}$AT colocalized to the apical membrane of enterocytes (Fig. 7). In accordance to the findings for mRNA and protein levels of rBAT and $b^{\circ,+}$AT, their immunoreactivity was strongest in ileum and very weak in duodenum and showed a similar gradient of expression along the villi as seen for the basolateral amino acid transporter subunits.

Discussion

Amino acid absorption in the small intestine represents a major source of amino acids for organ and cellular functions. Correspondingly, a wide variety of amino acid transport systems is expressed in the small intestine epithelium on both the apical brush border membrane and the basolateral side (Munck, 1995; Palacin *et al.* 1998). The recent identification of the important heteromeric amino acid transporter family has made it possible to correlate existing functional data with the expression and localization of specific transporters. Heteromeric amino acid transporters are widely expressed in epithelial and non-epithelial cells, and distinct patterns of mRNA tissue distribution suggested that some members of this family such as LAT2, y^+-LAT1 and $b^{\circ,+}$AT are predominantly expressed in epithelia such as those of kidney and small intestine (Chillaron *et al.* 2001; Wagner *et al.* 2001; Broer, 2002; Verrey *et al.* 2004). The present study investigated, in mouse intestine, the segmental expression pattern and relative abundance of heteromeric amino acid transporter subunit mRNAs and proteins, as well as their protein subcellular localization.

In agreement with previous studies characterizing functionally amino acid transport systems in the apical brush border membrane, both subunits of system $b^{\circ,+}$, rBAT and $b^{\circ,+}$AT, were detected in small intestine on mRNA and protein levels and localized to the apical membrane (Rosenberg *et al.* 1967; Furlong & Stiel, 1993; Munck, 1995; Munck *et al.* 2000; Torras-Llort *et al.* 2001). mRNA and protein showed a distinct segmental expression pattern with a gradual increase from the duodenum to the ileum that corresponds to previous functional descriptions (Munck, 1995). However, the
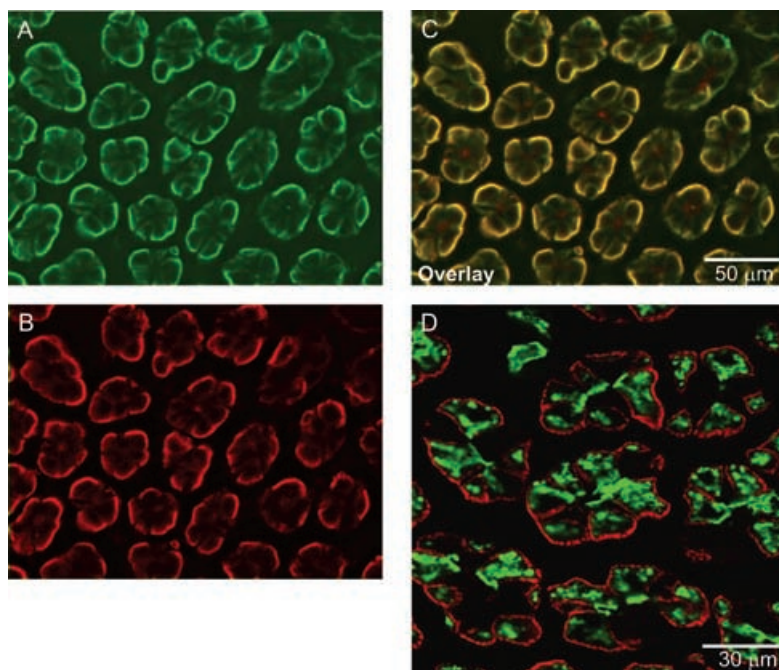

Figure 4. Localization of 4F2hc and LAT2 in mouse stomach

A–C, immunohistochemical labelling localized 4F2hc (green, *A*) and LAT2 (red, *B*) to the basolateral side of large cells along the gastric gland. *D*, staining of the parietal cell specific β-subunit of the gastric H^+/K^+-ATPase (green) identifies the cells expressing LAT2 as acid-secreting parietal cells. Original magnification 400×.

parallel expression of rBAT and $b^{o,+}$AT along the small intestine contrasts with the opposed gradients observed in kidney proximal tubule (Pfeiffer *et al.* 1999). We hypothesize that the putative additional rBAT-associated protein expressed in the distal part of the proximal tubule is not expressed in the small intestine (Pfeiffer *et al.* 1999; Fernandez *et al.* 2002). Along the villi, a gradient of expression was observed by immunohistochemistry with a higher amount on the tips where most of the absorptive transport processes take place. In the crypts between the villi, only a weak signal was found for all

amino acid transporter subunits suggesting that the full expression of these transporters is only acquired during maturation and concomitant migration of enterocytes. The localization of both rBAT and $b^{o,+}$AT subunits in the small intestine also explains the defect in cystine and dibasic amino acid absorption observed in patients with cystinuria (Rosenberg *et al.* 1965, 1966; Furlong & Stiel, 1993; Palacin *et al.* 2001). Mutations in either subunit can cause cystinuria, a disease primarily characterized by the renal loss of cystine and dibasic amino acids and the subsequent formation of cystine kidney stones and kidney
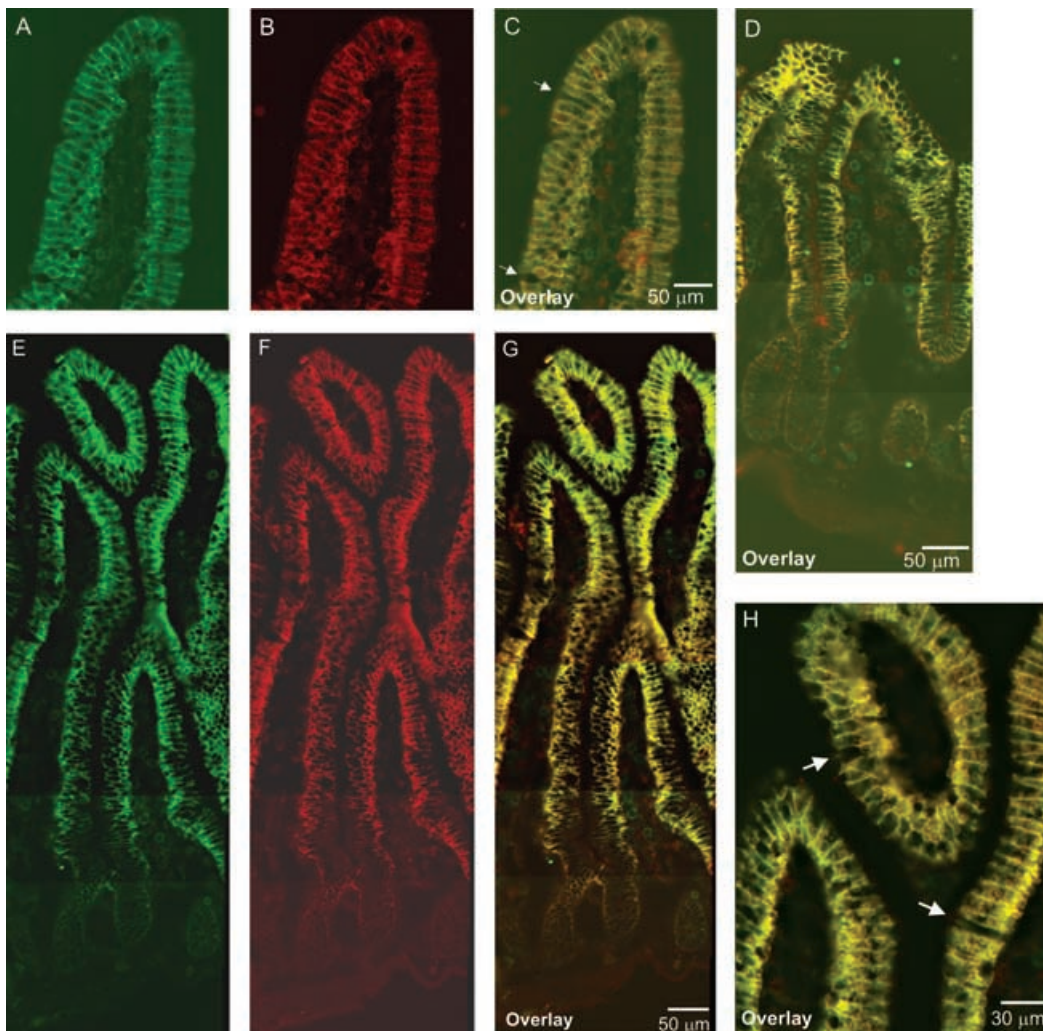

Figure 5. Localization of 4F2hc and LAT2 in mouse small intestine
Immunohistochemistry localized 4F2hc (green) and LAT-2 (red) to the basolateral side of the epithelial cells lining the duodenum, jejunum and ileum. 4F2hc and LAT2 colocalized and showed a gradient of expression along the villi with higher expression in the tips. *A* and *B*, 4F2hc and LAT2 localization in mouse duodenum; *C*, overlay of 4F2hc and LAT2 (yellow). Arrows show single dispersed cells which did not show staining for 4F2 and LAT2. *D*, colocalization of 4F2hc and LAT2 in jejunum, overlay (yellow). *E–G*, localization of 4F2hc and LAT2 in ileum and overlay (yellow). Original magnifications 400×. *H*, higher magnification of overlay of 4F2hc and LAT2 in ileum showing colocalization of both subunits to the basolateral membrane and some vesicular intracellular structures. Note that some cells were not stained for 4F2 and LAT2 (arrows). Original magnification 600×.
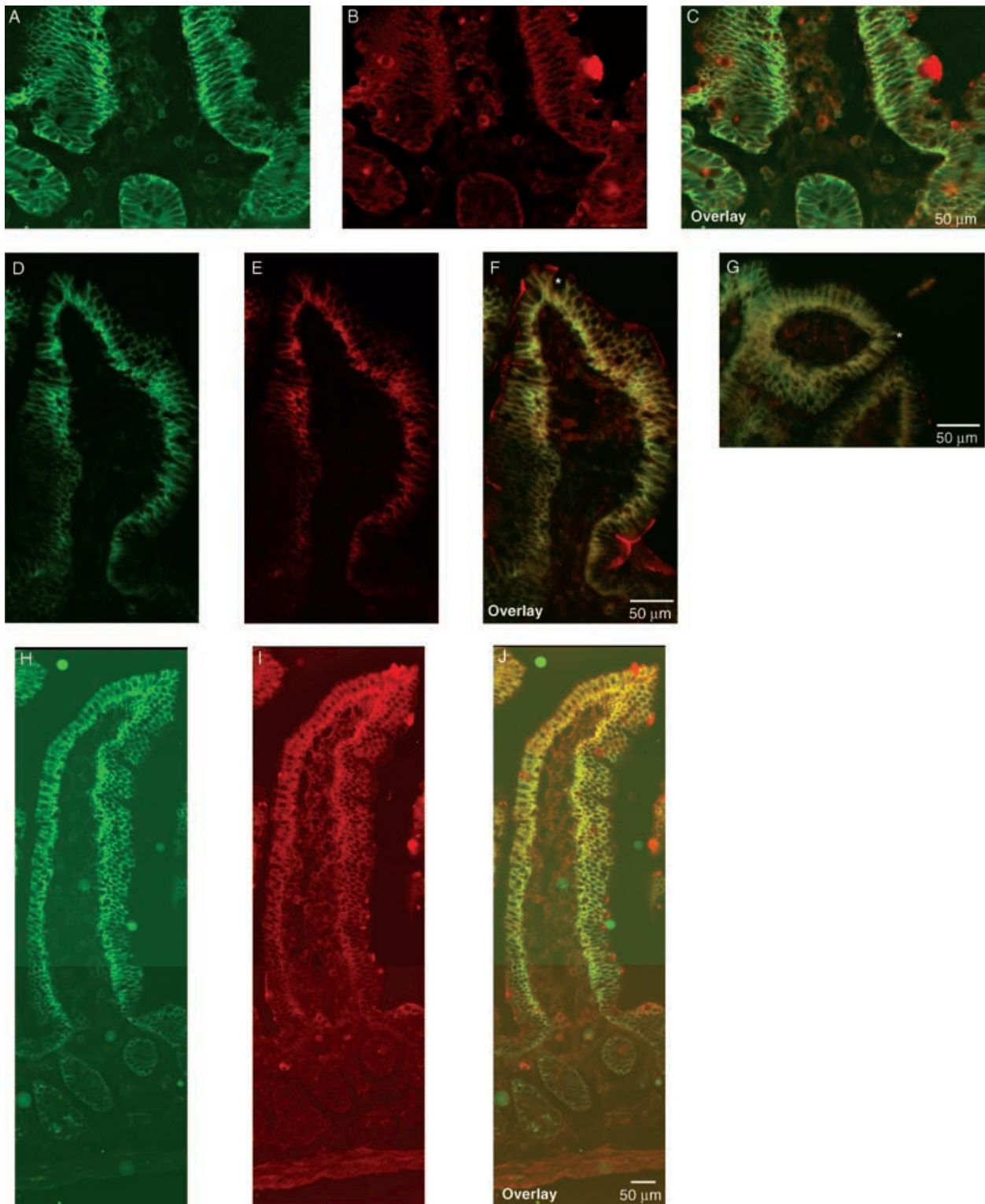
Figure 6. Localization of 4F2hc and y$^+$-LAT1 in mouse intestine
y$^+$-LAT1 (red) colocalized with 4F2hc (green) in duodenum, jejunum and ileum to the basolateral side of the epithelial cells. *A–C*, only a weak signal for y$^+$-LAT1 was seen in duodenum. *D–J*, similar to LAT2 a gradient of expression was seen for y$^+$-LAT1 along the villi of the jejunum (*D–I*) and ileum (*H–J*). The red staining appearing in the lumen (*E* and *F*) may result from unspecific antibody binding to mucus and was also seen with pre-immune serum. Note that not all cells were stained for 4F2hc and y$^+$-LAT1 as marked by the asterisk; these cells most likely represent goblet cells. No staining for y$^+$-LAT1 was seen in stomach and colon. Original magnification 400×.

destruction. The fact that patients with cystinuria do not suffer from malnutrition (Palacin *et al.* 2001) is most likely explained by the presence of peptide transporters which can transport small di- and tripeptides containing dibasic amino acids, and by the fact that the reduced form of cystine, L-cysteine, can be transported by other transporters and is not an essential amino acid.

The localization of the system L transporter LAT2 and the y^+L transporter y^+-LAT1 on the basolateral side of small intestine enterocytes confirms previous data describing functionally such amino acid transport activities in basolateral membranes (Desjeux *et al.* 1980; Lash & Jones, 1984; Wilde & Kilberg, 1991). In addition, localization of y^+-LAT1 on the basolateral side of enterocytes and its predominant expression in jejunum and ileum corresponds to the localization of defective lysine fluxes across the basolateral membrane

of enterocytes in jejunum of patients with lysinuric protein intolerance (LPI) (Desjeux *et al.* 1980). LPI is caused by mutations in the y^+-LAT1 encoding gene *SLC7A7* and is characterized by the defective transport of dibasic amino acids across the basolateral membrane of kidney proximal tubules and small intestine (Borsani *et al.* 1999; Torrents *et al.* 1999; Simell, 2001). The consequent reduction in blood arginine levels leads to impairment of the urea cycle, hyperammonaemia, failure to thrive, hepatosplenomegaly, osteoporosis, pulmonary problems (alveolar proteinosis) and mental deterioration (Simell, 2001). Apparently, the loss of y^+-LAT1 function as main basolateral efflux pathway of dibasic amino acids into the extracellular space and blood cannot be fully compensated by other transporters such as cationic amino acid transporters (system y^+). To date, the pattern of expression and localization of system y^+ amino acid transporters in
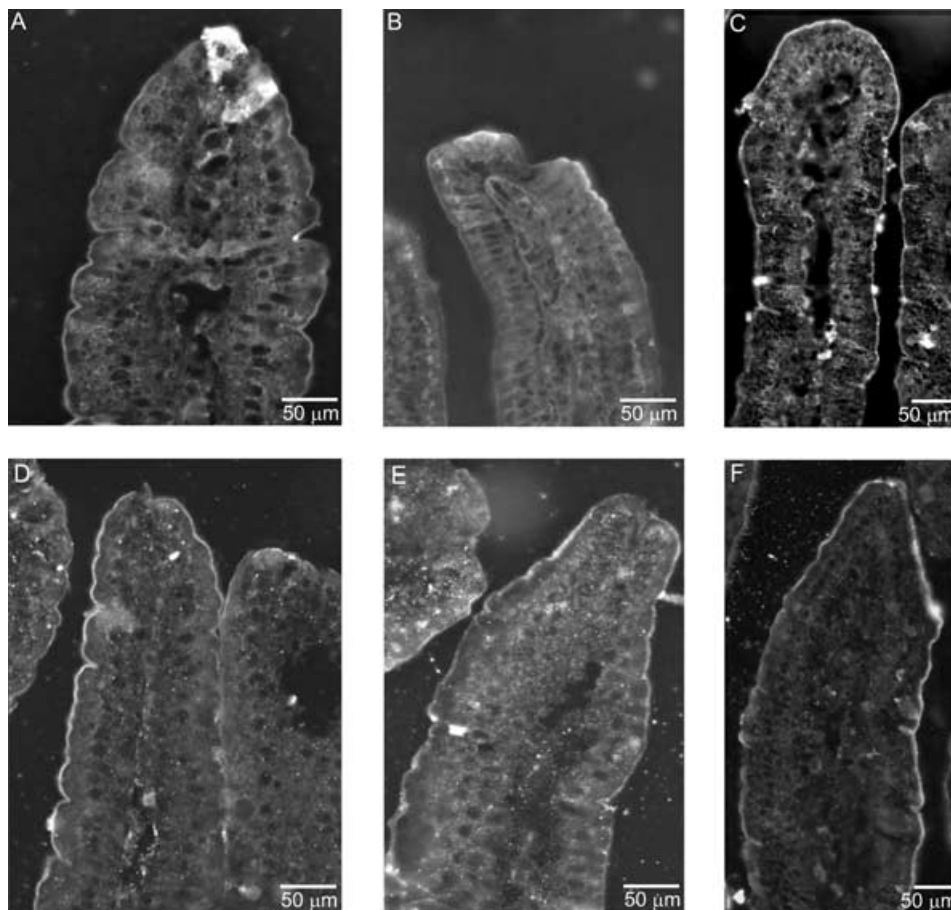

Figure 7. Localization of rBAT and its light chain b$^{\circ,+}$AT in mouse intestine
Both rBAT (upper panel) and b$^{\circ,+}$AT (lower panel) were found in the apical membrane of the epithelial cells lining the duodenum (*A* and *D*), jejunum (*B* and *E*) and ileum (*C* and *F*). In duodenum and jejunum, only a weak staining was found for rBAT, whereas the strongest staining was seen for both subunits in ileum. Original magnification 400×.

the intestine has not been reported. Both y^+-LAT1 and LAT2 showed the same gradual expression pattern along the villi as seen also for rBAT and $b^{\circ,+}$AT, suggesting that these transporters may cooperate in vectorial transport of amino acids from the intestinal lumen to the blood as described similarly in the kidney (Bauch *et al.* 2003). Interestingly, LAT2 shows a slightly different segmental gradient of expression than y^+-LAT1, rBAT and $b^{\circ,+}$AT. LAT2 expression peaked in the jejunum whereas the other light subunits in the ileum. Whereas the heavy chain rBAT followed the expression of its light subunit $b^{\circ,+}$AT, 4F2hc was widely expressed along the intestine covering the expression of its several associated light chains.

The expression of the basolateral 'absorptive transporter' LAT2 in the acid-secretory parietal cells of mouse stomach is surprising as the stomach is not thought to participate in amino acid absorption and is not known to express apical uptake pathways for amino acids. However, uptake of phenylalanine and leucine into isolated parietal cells has been observed that resembles system L transport activity (Sobrevia *et al.* 1992). Thus, LAT2 may play another role in parietal cells, for instance taking part in the uptake of amino acids that are used for ATP synthesis. Alternatively, LAT2 may also be involved in the stimulation of acid secretion by a protein rich diet that increases blood amino acid levels (Varner *et al.* 1980).

The expression of the xCT subunit in stomach points to another requirement for amino acids in gastric physiology, as cystine uptake mediated by xCT is essential for glutathione (GSH) synthesis. GSH has been shown to play a major protective role against radicals in intestine and to be taken up by cells that are not able to synthesize it. The expression of xCT is directly linked to glutathione synthesis and cystine uptake by xCT even represents the rate-limiting step for GSH synthesis in a variety of other cells (Sagara *et al.* 1993; Sato *et al.* 1995, 2001). The cellular localization of xCT in mouse stomach could not be determined because of the lack of specific antibodies.

Very little expression of the LAT1 and Asc-1 subunits was found in the intestine. LAT1 was found essentially in brain, as previously described (Wagner *et al.* 2001; Verrey *et al.* 2004), to some extent in stomach and at very low levels in ileum, colon, liver and kidney. The mRNA of the Asc-1 subunit was found only in brain and not in intestine, liver and kidney. A previous report has indicated the presence of a 4.4 kb RNA in small intestine instead of the 1.9 kb RNA in brain (Fukasawa *et al.* 2000). However, the significance of this 4.4 kb RNA remains to be established.

In summary, several subunits of the novel family of heteromeric amino acid transporters are expressed along the mouse intestine with distinct patterns and subcellular localizations. The high expression level and the polarized localization of the subunits forming the apical cystine transporter ($b^{\circ,+}$AT–rBAT) and the basolateral systems y^+L and L (y^+-LAT1–4F2hc and LAT2–4F2hc) point to an important role of these transporters in normal intestinal amino acid absorption and is in agreement with previous functional studies describing such amino acid transport systems. In addition, the localization of the disease-causing subunits rBAT, $b^{\circ,+}$AT and y^+-LAT1 fully explains the intestinal phenotype seen in patients with cystinuria and lysinuric protein intolerance. The expression of amino acid transporters in stomach requires further experiments to elucidate their role in gastric physiology.

References

Avissar NE, Ryan CK, Ganapathy V & Sax HC (2001). Na$^+$-dependent neutral amino acid transporter ATB^0 is a rabbit epithelial cell brush-border protein. *Am J Physiol Cell Physiol* **281**, C963–C971.

Bauch C, Forster N, Loffing-Cueni D, Summa V & Verrey F (2003). Functional cooperation of epithelial heteromeric amino acid transporters expressed in MDCK cells. *J Biol Chem* **278**, 1316–1322.

Borsani G, Bassi MT, Sperandeo MP, De Grandi A, Buoninconti A, Riboni M, Manzoni M, Incerti B, Pepe A, Andria G, Ballabio A & Sebastio G (1999). SLC7A7, encoding a putative permease-related protein, is mutated in patients with lysinuric protein intolerance. *Nat Genet* **21**, 297–301.

Broer S (2002). Adaptation of plasma membrane amino acid transport mechanisms to physiological demands. *Pflugers Arch* **444**, 457–466.

Calonge MJ, Gasparini P, Chillaron J, Chillon M, Gallucci M, Rousaud F, Zelante L, Testar X, Dallapiccola B, Di Silverio F, Barcelo P, Estivill X, Zorzano A, Nunes V & Palacin M (1994). Cystinuria caused by mutations in rBAT, a gene involved in the transport of cystine. *Nat Genet* **6**, 420–425.

Campbell WA, Sah DE, Medina MM, Albina JE, Coleman WB & Thompson NL (2000). TA1/LAT-1/CD98 light chain and system L activity, but not 4F2/CD98 heavy chain, respond to arginine availability in rat hepatic cells. Loss of response in tumor cells. *J Biol Chem* **275**, 5347–5354.

Chen Z, Fei YJ, Anderson CM, Wake KA, Miyauchi S, Huang W, Thwaites DT & Ganapathy V (2003). Structure, function and immunolocalization of a proton-coupled amino acid transporter (hPAT1) in the human intestinal cell line Caco-2. *J Physiol* **546**, 349–361.

Chillaron J, Estevez R, Mora C, Wagner CA, Suessbrich H, Lang F, Gelpi JL, Testar X, Busch AE, Zorzano A & Palacin M (1996). Obligatory amino acid exchange via systems $b^{\circ,+}$-like and y^+1-like. A tertiary active transport mechanism for renal reabsorption of cystine and dibasic amino acids. *J Biol Chem* **271**, 17761–17770.

Chillaron J, Roca R, Valencia A, Zorzano A & Palacin M (2001). Heteromeric amino acid transporters: biochemistry, genetics, and physiology. *Am J Physiol Renal Physiol* **281**, F995–F1018.

Daniel H & Rubio-Aliaga I (2003). An update on renal peptide transporters. *Am J Physiol Renal Physiol* **284**, F885–F892.

Desjeux JF, Simell RO, Dumontier AM & Perheentupa J (1980). Lysine fluxes across the jejunal epithelium in lysinuric protein intolerance. *J Clin Invest* **65**, 1382–1387.

Feliubadalo L, Font M, Purroy J, Rousaud F, Estivill X, Nunes V, Golomb E, Centola M, Aksentijevich I, Kreiss Y, Goldman B, Pras M, Kastner DL, Pras E, Gasparini P, Bisceglia L, Beccia E, Gallucci M, de Sanctis L, Ponzone A, Rizzoni GF, Zelante L, Bassi MT, George AL Jr & Palacin M, (1999). International Cystinuria Consortium. Non-type I cystinuria caused by mutations in SLC7A9, encoding a subunit ($b^{o,+}$AT) of rBAT. *Nat Genet* **23**, 52–57.

Fernandez E, Carrascal M, Rousaud F, Abian J, Zorzano A, Palacin M & Chillaron J (2002). rBAT-$b^{0,+}$AT heterodimer is the main apical reabsorption system for cystine in the kidney. *Am J Physiol Renal Physiol* **283**, F540–F548.

Fukasawa Y, Segawa H, Kim JY, Chairoungdua A, Kim DK, Matsuo H, Cha SH, Endou H & Kanai Y (2000). Identification and characterization of a Na^+-independent neutral amino acid transporter that associates with the 4F2 heavy chain and exhibits substrate selectivity for small neutral D- and L-amino acids. *J Biol Chem* **275**, 9690–9698.

Furlong TJ & Stiel D (1993). Decreased uptake of L-cystine by duodenal brush border membrane vesicles from patients with cystinuria. *Aust N Z J Medical* **23**, 258–263.

Groneberg DA, Doring F, Eynott PR, Fischer A & Daniel H (2001). Intestinal peptide transport: ex vivo uptake studies and localization of peptide carrier PEPT1. *Am J Physiol Gastrointest Liver Physiol* **281**, G697–G704.

Lash LH & Jones DP (1984). Characteristics of cysteine uptake in intestinal basolateral membrane vesicles. *Am J Physiol Gastrointest Liver Physiol* **247**, G394–G401.

Loffing J, Zecevic M, Feraille E, Kaissling B, Asher C, Rossier BC, Firestone GL, Pearce D & Verrey F (2001). Aldosterone induces rapid apical translocation of ENaC in early portion of renal collecting system: possible role of SGK. *Am J Physiol Renal Physiol* **280**, F675–F682.

McLean IW & Nakane PK (1974). Periodate-lysine-paraformaldehyde fixative. A new fixation for immunoelectron microscopy. *J Histochem Cytochem* **22**, 1077–1083.

Meier C, Ristic Z, Klauser S & Verrey F (2002). Activation of system L heterodimeric amino acid exchangers by intracellular substrates. *EMBO J* **21**, 580–589.

Munck LK (1995). Chloride-dependent amino acid transport in the small intestine: occurrence and significance. *Biochim Biophys Acta* **1241**, 195–213.

Munck LK, Grondahl ML, Thorboll JE, Skadhauge E & Munck BG (2000). Transport of neutral, cationic and anionic amino acids by systems B, $b^{0,+}$, X_{AG}, and ASC in swine small intestine. *Comp Biochem Physiol A Mol Integr Physiol* **126**, 527–537.

Munck BG & Munck LK (1999). Effects of pH changes on systems ASC and B in rabbit ileum. *Am J Physiol* **276**, G173–G184.

Palacin M, Estevez R, Bertran J & Zorzano A (1998). Molecular biology of mammalian plasma membrane amino acid transporters. *Physiol Rev* **78**, 969–1054.

Palacin M, Goodyer P, Nunes V & Gasparini P (2001). Cystinuria. In *The Metabolic and Molecular Bases of Inherited Disease*, ed. Scriver CR, Beaudet AL, Sly WS, Valle D, pp. 4909–4932. McGraw-Hill, New York.

Palacin M & Kanai Y (2004). The ancillary proteins of HATs: SLC3 family of amino acid transporters. *Pflugers Arch* **447**, 490–494.

Pfeiffer R, Loffing J, Rossier G, Bauch C, Meier C, Eggermann T, Loffing-Cueni D, Kühn LC & Verrey F (1999). Luminal heterodimeric amino acid transporter defective in cystinuria. *Mol Biol Cell* **10**, 4135–4147.

Rosenberg LE, Crawhall JC & Segal S (1967). Intestinal transport of cystine and cysteine in man: evidence for separate mechanisms. *J Clin Invest* **46**, 30–34.

Rosenberg LE, Downing S, Durant JL & Segal S (1966). Cystinuria: biochemical evidence for three genetically distinct diseases. *J Clin Invest* **45**, 365–371.

Rosenberg LE, Durant JL & Holland JM (1965). Intestinal absorption and renal extraction of cystine and cysteine in cystinuria. *N Engl J Med* **273**, 1239–1245.

Rossier G, Meier C, Bauch C, Summa V, Sordat B, Verrey F & Kühn LC (1999). LAT2, a new basolateral 4F2hc/CD98-associated amino acid transporter of kidney and intestine. *J Biol Chem* **274**, 34948–34954.

Sagara JI, Miura K & Bannai S (1993). Maintenance of neuronal glutathione by glial cells. *J Neurochem* **61**, 1672–1676.

Sato H, Fujiwara K, Sagara J & Bannai S (1995). Induction of cystine transport activity in mouse peritoneal macrophages by bacterial lipopolysaccharide. *Biochem J* **310**, 547–551.

Sato H, Kuriyama-Matsumura K, Hashimoto T, Sasaki H, Wang H, Ishii T, Mann GE & Bannai S (2001). Effect of oxygen on induction of the cystine transporter by bacterial lipopolysaccharide in mouse peritoneal macrophages. *J Biol Chem* **276**, 10407–10412.

Simell O (2001). Lysinuric protein intolerance and other cationic aminoacidurias. In *The Metabolic and Molecular Bases of Inherited Disease*, ed. Scriver CR, Beaudet AL, Sly WS, Valle D, pp. 4933–4956. McGraw-Hill, New York.

Sobrevia L, Medina V, Reinicke K & Bravo I (1992). Uptake of L-leucine and L-phenylalanine across the basolateral cell surface in isolated oxyntic glands. *Biochim Biophys Acta* **1106**, 257–263.

Torras-Llort M, Torrents D, Soriano-Garcia JF, Gelpi JL, Estevez R, Ferrer R, Palacin M & Moreto M (2001). Sequential amino acid exchange across b$^{0,+}$-like system in chicken brush border jejunum. *J Membr Biol* **180**, 213–220.

Torrents D, Mykkanen J, Pineda M, Feliubadalo L, Estevez R, de Cid R, Sanjurjo P, Zorzano A, Nunes V, Huoponen K, Reinikainen A, Simell O, Savontaus ML, Aula P & Palacin M (1999). Identification of SLC7A7, encoding y$^+$LAT-1, as the lysinuric protein intolerance gene. *Nat Genet* **21**, 293–296.

Varner AA, Isenberg JI, Elashoff JD, Lamers CB, Maxwell V & Shulkes AA (1980). Effect of intravenous lipid on gastric acid secretion stimulated by intravenous amino acids. *Gastroenterology* **79**, 873–876.

Verrey F, Closs EI, Wagner CA, Palacin M, Endou H & Kanai Y (2004). CATs and HATs: the SLC7 family of amino acid transporters. *Pflugers Arch* **447**, 532–542.

Verrey F, Meier C, Rossier G & Kühn LC (2000). Glycoprotein-associated amino acid exchangers: broadening the range of transport specificity. *Pflugers Arch* **440**, 503–512.

Wagner CA, Finberg KE, Stehberger PA, Lifton RP, Giebisch GH, Aronson PS & Geibel JP (2002). Regulation of the expression of the Cl$^-$/anion exchanger pendrin in mouse kidney by acid-base status. *Kidney Int* **62**, 2109–2117.

Wagner CA, Lang F & Broer S (2001). Function and structure of heterodimeric amino acid transporters. *Am J Physiol Cell Physiol* **281**, C1077–C1093.

Wilde SW & Kilberg MS (1991). Glutamine transport by basolateral plasma-membrane vesicles prepared from rabbit intestine. *Biochem J* **277**, 687–691.

Acknowledgements

Supplementary material

The online version of this paper can be accessed online at: DOI: 10.1113/jphysiol.2004.065037
http://jp.physoc.org/cgi/content/full/jphysiol.2004.065037v1/DC1 and contains supplementary material consisting of two figures.
This material is additionally available at:
http://blackwellpublishing.com/products/journals/suppmat/tjp/tjp344/tjp344sm.htm